

Vibrational and Rotational Spectral Data for Possible Interstellar Detection of AlH_3OH_2 , SiH_3OH , and SiH_3NH_2

A. G. Watrous,¹ B. R. Westbrook,¹ M. C. Davis¹ and Ryan C. Fortenberry^{1*}

¹*Department of Chemistry & Biochemistry, University of Mississippi, University, MS 38677-1848, US*

Accepted XXX. Received YYY; in original form ZZZ

ABSTRACT

This work provides the first full set of vibrational and rotational spectral data needed to aid in the detection of AlH_3OH_2 , SiH_3OH , and SiH_3NH_2 in astrophysical or simulated laboratory environments through the use of quantum chemical computations at the CCSD(T)-F12b level of theory employing quartic force fields for the three molecules of interest. Previous work has shown that SiH_3OH and SiH_3NH_2 contain some of the strongest bonds of the most abundant elements in space. AlH_3OH_2 also contains highly abundant atoms and represents an intermediate along the reaction pathway from H_2O and AlH_3 to AlH_2OH . All three of these molecules are also polar with AlH_3OH_2 having the largest dipole of 4.58 D and the other two having dipole moments in the 1.10–1.30 D range, large enough to allow for the detection of these molecules in space through rotational spectroscopy. The molecules also have substantial infrared intensities with many of the frequencies being over 90 km mol^{-1} and falling within the currently uncertain 12–17 μm region of the spectrum. The most intense frequency for AlH_3OH_2 is ν_9 which has an intensity of 412 km mol^{-1} at 777.0 cm^{-1} (12.87 μm). SiH_3OH has an intensity of 183 km mol^{-1} at 1007.8 cm^{-1} (9.92 μm) for ν_5 , and SiH_3NH_2 has an intensity of 215 km mol^{-1} at 1000.0 cm^{-1} (10.00 μm) for ν_7 .

Key words: astrochemistry – molecular data – molecular processes – ISM: molecules – infrared: ISM – radio lines: ISM

1 INTRODUCTION

Extraterrestrial Al–O bonds have been found in the form of AlOH and AlO in evolved stars and in the atmosphere of the exoplanet WASP-43b (Tenenbaum & Ziurys 2009, 2010; Takigawa et al. 2017; Chubb et al. 2020). Additionally, silicon monoxide (SiO) has been found in Sagittarius B2 (Wilson et al. 1971), but the astronomical literature has not reported any other small molecule detections containing an Si–O bond (McGuire et al. 2018). However, crystalline compounds containing silicon and oxygen, such as enstatite (MgSiO_3), have been spectroscopically observed toward NGC 6302 (Molster et al. 2001, 2002) with most of the spectral data falling in the range of 17–50 μm . In contrast, the 2.4–12 μm range of the spectrum is mostly attributed to carbon molecules such as polycyclic aromatic hydrocarbons (PAHs) (Molster et al. 2001). Despite the typical attribution of this region to carbonaceous PAHs, there are still many unknowns in the observed spectra that may be filled by other Si containing molecules. In particular, spectral data has many peaks from 12–17 μm that correspond to unknown molecules, but this “uncertain part of the spectra” (Molster et al. 2001) is in the range of many vibrational features for known Si structures (Molster et al. 2001, 2002). Hence, other Si containing molecules may yet be observed in that region. Additionally, oxygen rich stars do not have nearly as strong of PAH features allowing for Si containing molecules with strong vibrational features to be detected there (Molster et al. 2002).

Past work on inorganic oxides and related hydrides, including

$(\text{MO})_2$ with $\text{M} = \text{Al}$ and Si , have been found to have anharmonic frequencies below 20 μm (500 cm^{-1}) (Westbrook & Fortenberry 2020). Most of the M–O bond frequencies fall within the range of the unclear area of IR spectra, and the metal oxides have intensities of over 50 km mol^{-1} for about half of the frequencies. Due to the number of frequencies in a small range within this region, the intensities of the frequencies need to be relatively strong to stand out from the forest of lines. Additionally, the metal oxides and related hydrides previously mentioned have similar features to large, crystalline forms of Si containing molecules such as enstatite and forsterite (Mg_2SiO_4), both of which have been detected in space (Molster et al. 2001, 2002). Enstatite and forsterite monomers have also been reported to exhibit infrared intensities over 200 km mol^{-1} which is a large enough intensity for the frequencies of these molecules to stand out from the spectral features of other molecules (Valencia et al. 2020). Consequently, this is a promising spectral region in which to look for other silicon containing molecules.

Previous work has also shown that oxygen and nitrogen form bonds with aluminum and silicon that are stronger than nearly any others in the first three rows of the periodic table (Doerksen & Fortenberry 2020). Of these aforementioned strong bonds, aluminum and oxygen form the strongest bond followed by silicon and oxygen. As such, AlH_2OH and AlH_2NH_2 have been previously studied computationally and have shown promise for interstellar detection due to their large dipole moments and intense vibrational frequencies (Watrous et al. 2021). Additionally, a previously computed exothermic pathway has shown that H_2O reacts with a simple aluminum hydride (AlH_3) molecule to produce AlH_2OH which could easily form in

* E-mail: r410@olemiss.edu

atmospheres of massive stars. This is due to the abundance of water (McGuire et al. 2018) and the perceived presence of AlH_3 which is likely unobserved because of its lack of a permanent dipole moment (Swinnen et al. 2009). AlH_3OH_2 has been previously computed to be an intermediate formed barrierlessly along this reaction pathway and has an energy lower than the starting reactants (Swinnen et al. 2009). For AlH_3OH_2 to persist on its own instead of serving as a short-lived intermediate, it will have to dissipate the excess energy from its formation by emission in the infrared. Such emission will make the infrared spectral data provided herein invaluable for a potential astronomical detection. Regardless, if this molecule is found in space, then AlH_3 and H_2O would also likely be present in the gas phase, allowing the detection of AlH_3OH_2 to provide evidence for the presence of the otherwise difficult-to-observe AlH_3 molecule. SiH_3OH and SiH_3NH_2 are related molecules of interest given the chemical similarity of Si and Al and the strength of bonds between Si and N or O. Not only does silicon form strong bonds with oxygen (Doerksen & Fortenberry 2020), but it also is the third most abundant element in the earth’s mantle after oxygen and magnesium, making it a potential component in the formation of planets from dust grains.

To that end, this work utilizes quantum chemical methods to compute optimized structures, energies, and spectroscopic data for AlH_3OH_2 , SiH_3OH , and SiH_3NH_2 . The latter two containing Si have relatively strong bonds of at least $-91.10 \text{ kcal mol}^{-1}$ (Doerksen & Fortenberry 2020), and all three contain highly abundant atoms (Savage & Sembach 1996). The Al-O bond in AlH_3OH_2 is dative in nature but still has an energy of more than 17 kcal mol^{-1} (Swinnen et al. 2009) making it usable with the present methods. None of the three molecules has yet been detected in space, and neither AlH_3OH_2 nor SiH_3OH have been examined experimentally via gas-phase infrared spectroscopy in the laboratory. On the other hand, SiH_3NH_2 has been previously observed in the infrared (Beach 1992), offering some gas-phase experimental data to benchmark the present computational work. However, there are still holes in the spectral interpretation that remain to be elucidated.

Theoretical spectral data can be provided at a reasonable balance between accuracy and computational cost by quartic force fields (QFFs), which are a fourth-order Taylor series expansions of the internuclear potential term of the Watson Hamiltonian (Fortenberry & Lee 2019). QFFs based on coupled cluster theory at the singles, doubles, and perturbative triples level within the explicitly correlated F12b construction [CCSD(T)-F12b] and with the corresponding cc-pVTZ-F12 basis set (Raghavachari et al. 1989; Shavitt & Bartlett 2009; Crawford & Schaefer III 2000; Peterson et al. 2008; Yousaf & Peterson 2008) typically produce fundamental vibrational frequencies within 5 to 7 cm^{-1} of gas-phase experiments (Agbaglo & Fortenberry 2019a,b). This level of accuracy is sufficient enough to lend theoretical support to NASA missions such as the *Stratospheric Observatory for Infrared Astronomy* (SOFIA) or the upcoming *James Webb Space Telescope* (JWST).

2 COMPUTATIONAL DETAILS

The geometry optimizations, harmonic frequencies, single point energies, and dipole moments are computed using the Molpro 2015.1 (Werner et al. 2015) and Molpro 2020.1 software packages (Werner et al. 2020) at the CCSD(T)-F12b/cc-pVTZ-F12 (Adler et al. 2007; Peterson et al. 2008; Yousaf & Peterson 2008; Knizia et al. 2009) level of theory. This will be referred to as F12-TZ. The MP2/aug-cc-pVTZ double-harmonic intensities are computed using the Gaussian16 program (Møller & Plesset 1934; Frisch et al. 2016; Kendall et al. 1992).

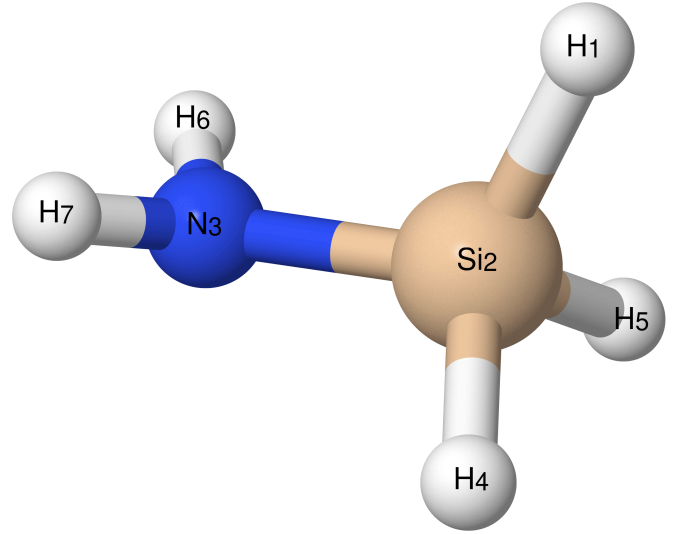


Figure 1. Visual depiction of the SiH_3NH_2 structure

Each molecular geometry is first optimized at the F12-TZ level of theory. This geometry is then displaced by 0.005 \AA or 0.005 radians along the symmetry-internal coordinates to form the QFFs.

The QFF for SiH_3NH_2 is composed of 19585 points and is defined by the coordinate system below, with atom labels corresponding to Figure 1.

$$S_1(a') = r(\text{H}_1 - \text{Si}_2) \quad (1)$$

$$S_2(a') = r(\text{Si}_2 - \text{N}_3) \quad (2)$$

$$S_3(a') = \frac{1}{\sqrt{2}} [r(\text{Si}_2 - \text{H}_4) + r(\text{Si}_2 - \text{H}_5)] \quad (3)$$

$$S_4(a') = \frac{1}{\sqrt{2}} [r(\text{N}_3 - \text{H}_6) + r(\text{N}_3 - \text{H}_7)] \quad (4)$$

$$S_5(a') = \angle(\text{H}_1 - \text{Si}_2 - \text{N}_3) \quad (5)$$

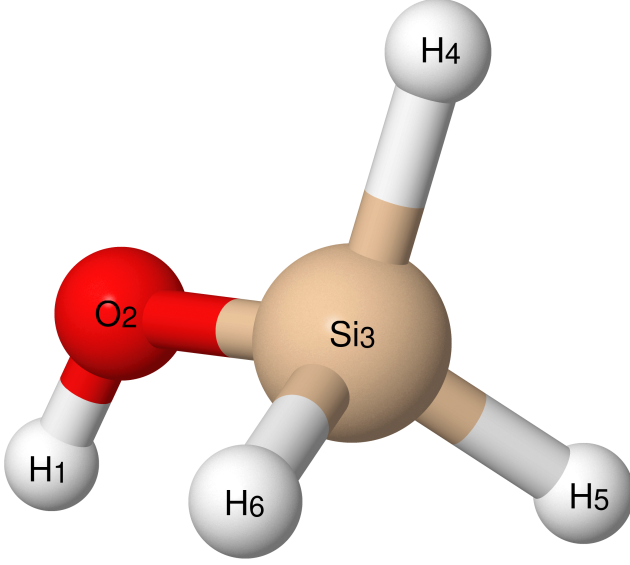
$$S_6(a') = \frac{1}{\sqrt{2}} [\angle(\text{H}_5 - \text{Si}_2 - \text{N}_3) + \angle(\text{H}_4 - \text{Si}_2 - \text{N}_3)] \quad (6)$$

$$S_7(a') = \frac{1}{\sqrt{2}} [\angle(\text{H}_6 - \text{N}_3 - \text{Si}_2) + \angle(\text{H}_7 - \text{N}_3 - \text{Si}_2)] \quad (7)$$

$$S_8(a') = \frac{1}{\sqrt{2}} [\tau(\text{H}_1 - \text{Si}_2 - \text{N}_3 - \text{H}_6) - \tau(\text{H}_1 - \text{Si}_2 - \text{N}_3 - \text{H}_7)] \quad (8)$$

$$S_9(a') = \frac{1}{\sqrt{2}} [\tau(\text{H}_5 - \text{Si}_2 - \text{N}_3 - \text{H}_6) - \tau(\text{H}_4 - \text{Si}_2 - \text{N}_3 - \text{H}_7)] \quad (9)$$

$$S_{10}(a'') = \frac{1}{\sqrt{2}} [r(\text{Si}_2 - \text{H}_4) - r(\text{Si}_2 - \text{H}_5)] \quad (10)$$


 Figure 2. SiH₃OH

$$S_{11}(a'') = \frac{1}{\sqrt{2}} [r(\text{N}_3 - \text{H}_6) - r(\text{N}_3 - \text{H}_7)] \quad (11)$$

$$S_{12}(a'') = \frac{1}{\sqrt{2}} [\angle(\text{H}_5 - \text{Si}_2 - \text{N}_3) - \angle(\text{H}_4 - \text{Si}_2 - \text{N}_3)] \quad (12)$$

$$S_{13}(a'') = \frac{1}{\sqrt{2}} [\angle(\text{H}_6 - \text{N}_3 - \text{Si}_2) - \angle(\text{H}_7 - \text{N}_3 - \text{Si}_2)] \quad (13)$$

$$S_{14}(a'') = \frac{1}{\sqrt{2}} [\tau(\text{H}_1 - \text{Si}_2 - \text{N}_3 - \text{H}_6) + \tau(\text{H}_1 - \text{Si}_2 - \text{N}_3 - \text{H}_7)] \quad (14)$$

$$S_{15}(a'') = \frac{1}{\sqrt{2}} [\tau(\text{H}_5 - \text{Si}_2 - \text{N}_3 - \text{H}_6) + \tau(\text{H}_4 - \text{Si}_2 - \text{N}_3 - \text{H}_7)] \quad (15)$$

The coordinate system for AlH₃OH₂ is the same as SiH₃NH₂ above with Al in the place of Si and O in the place of N.

The coordinate system for SiH₃OH requires 8481 points and is defined in the following with atom labels corresponding to Figure 2.

$$S_1(a') = r(\text{H}_1 - \text{O}_2) \quad (16)$$

$$S_2(a') = r(\text{O}_2 - \text{Si}_3) \quad (17)$$

$$S_3(a') = r(\text{Si}_3 - \text{H}_4) \quad (18)$$

$$S_4(a') = \frac{1}{\sqrt{2}} [r(\text{Si}_3 - \text{H}_5) + r(\text{Si}_3 - \text{H}_6)] \quad (19)$$

$$S_5(a') = \angle(\text{H}_1 - \text{O}_2 - \text{Si}_3) \quad (20)$$

$$S_6(a') = \angle(\text{O}_2 - \text{Si}_3 - \text{H}_4) \quad (21)$$

$$S_7(a') = \frac{1}{\sqrt{2}} [\angle(\text{O}_2 - \text{Si}_3 - \text{H}_5) + \angle(\text{O}_2 - \text{Si}_3 - \text{H}_6)] \quad (22)$$

$$S_8(a') = \frac{1}{\sqrt{2}} [\tau(\text{H}_1 - \text{O}_2 - \text{Si}_3 - \text{H}_5) - \tau(\text{H}_1 - \text{O}_2 - \text{Si}_3 - \text{H}_6)] \quad (23)$$

$$S_9(a'') = \frac{1}{\sqrt{2}} [r(\text{Si}_3 - \text{H}_5) - r(\text{Si}_3 - \text{H}_6)] \quad (24)$$

$$S_{10}(a'') = \tau(\text{H}_1 - \text{O}_2 - \text{Si}_3 - \text{H}_4) \quad (25)$$

$$S_{11}(a'') = \frac{1}{\sqrt{2}} [\angle(\text{O}_2 - \text{Si}_3 - \text{H}_5) - \angle(\text{O}_2 - \text{Si}_3 - \text{H}_6)] \quad (26)$$

$$S_{12}(a'') = \frac{1}{\sqrt{2}} [\tau(\text{H}_1 - \text{O}_2 - \text{Si}_3 - \text{H}_5) + \tau(\text{H}_1 - \text{O}_2 - \text{Si}_3 - \text{H}_6)] \quad (27)$$

Following the computation of single point energies at each of these displaced geometries, the QFFs are generated by a least-squares fitting procedure where the sum of the squared residuals is on the order of 10⁻¹⁶ a.u.² or less for all molecules. This yields the equilibrium geometry, and a refit of the potential energy surface zeros the gradients and produces the new equilibrium geometry along with the corresponding force constants. The resulting force constants are transformed into Cartesian coordinates using the INTDER program (Allen & coworkers 2005) which are then used in second-order rotational and vibrational perturbation theory (Mills 1972) within the SPECTRO software package (Gaw et al. 1996) in order to calculate rovibrational spectral data (Watson 1977; Papoušek & Aliev 1982). Type-1 and 2 Fermi resonances, Fermi polyads (Martin & Taylor 1997), Coriolis resonances, and Darling-Dennison resonances are taken into account to increase the accuracy of the rovibrational data (Martin et al. 1995; Martin & Taylor 1997). The Fermi resonances for each molecule can be found in Table S2.

3 RESULTS AND DISCUSSION

3.1 Geometries and rotational constants

AlH₃OH₂ has the largest dipole moment out of the three molecules studied at 4.58 D. This dipole moment is stronger than other, similar aluminum and oxygen containing molecules such as AlH₂OH and

Table 1. Rotational constants and dipole moment of AlH_3OH_2 , SiH_3NH_2 , and SiH_3OH

Constant	Units	AlH_3OH_2	SiH_3NH_2	SiH_3OH
A_0	MHz	56168.1	68818.9	77174.6
B_0	MHz	9274.6	12646.5	13775.4
C_0	MHz	9130.9	12224.7	13553.9
Δ_J	kHz	23.495	11.122	13.574
Δ_K	kHz	165.768	359.365	463.425
Δ_{JK}	kHz	93.777	124.706	177.170
δ_J	Hz	474.202	467.870	255.285
δ_K	kHz	-544.657	-307.033	-658.864
Φ_J	mHz	-91.250	-2.035	-2.752
Φ_K	Hz	66.334	32.968	83.512
Φ_{JK}	Hz	24.203	6.555	23.787
Φ_{KJ}	Hz	-84.242	-28.812	-87.728
ϕ_j	μHz	-1768.830	-418.967	613.039
ϕ_{jk}	Hz	-8.133	-1.303	-2.708
ϕ_k	kHz	6.367	0.951	4.257
μ	D	4.58	1.21	1.29

Table 2. Vibrationally averaged and equilibrium geometrical parameters of AlH_3OH_2

	Units	Value
$R_0(\text{H}_1-\text{Al}_2)$	\AA	1.59197
$R_0(\text{Al}_2-\text{O}_3)$	\AA	2.04014
$R_0(\text{Al}_2-\text{H}_4)$	\AA	1.60154
$R_0(\text{O}_3-\text{H}_6)$	\AA	0.91884
$\angle_0(\text{Al}_2-\text{H}_1-\text{O}_3)$	deg	101.834
$\angle_0(\text{Al}_2-\text{H}_5-\text{O}_3)$	deg	96.206
$\angle_0(\text{O}_3-\text{H}_6-\text{Al}_2)$	deg	116.385
$R_e(\text{H}_1-\text{Al}_2)$	\AA	1.58742
$R_e(\text{Al}_2-\text{O}_3)$	\AA	2.02504
$R_e(\text{Al}_2-\text{H}_4)$	\AA	1.59756
$R_e(\text{O}_3-\text{H}_6)$	\AA	0.96189
$\angle_e(\text{Al}_2-\text{H}_1-\text{O}_3)$	deg	102.741
$\angle_e(\text{Al}_2-\text{H}_5-\text{O}_3)$	deg	95.695
$\angle_e(\text{O}_3-\text{H}_6-\text{Al}_2)$	deg	112.678

AIOH which have dipole moments of 1.22 and 1.11 D, respectively (Watrous et al. 2021; Fortenberry et al. 2020). SiH_3OH has the second largest dipole at 1.29 D which is much smaller than the dipole moment of AlH_3OH_2 . SiH_3NH_2 has a slightly smaller dipole moment still than SiH_3OH at 1.21 D. All three of these molecules have dipole moments large enough to be detectable in space through pure rotational spectroscopy, but AlH_3OH_2 does have a significantly larger dipole moment than the other two molecules. AlH_3OH_2 , SiH_3OH , and SiH_3NH_2 all show near-prolate character as indicated by their κ values of approximately -0.99 . Given this prolate nature, SiH_3OH and SiH_3NH_2 could be expected to have B_{eff} rotational constants comparable to their diatomic counterparts, SiO and SiN. However, in actuality the addition of the hydrogen atoms causes the rotational constants nearly to halve relative to the isolated diatomics (Huber & Herzberg 1979) and renders such a comparison moot. The principal rotational constants, quartic and sextic distortion coefficients, and dipole moments are reported in Table 1. The full set of equilibrium and first vibrationally excited rotational constants is shown in Table S1.

As shown in Table 2, AlH_3OH_2 has a heavy atom bond length of 2.03 \AA . This is longer than the Al-O bond in AlH_2OH and AIOH which are 1.70 and 1.68 \AA , respectively (Watrous et al. 2021; Forten-

Table 3. Vibrationally averaged and equilibrium geometrical parameters of SiH_3OH

	Units	Value
$R_0(\text{H}_1-\text{O}_2)$	\AA	0.92024
$R_0(\text{O}_2-\text{Si}_3)$	\AA	1.65312
$R_0(\text{Si}_3-\text{H}_4)$	\AA	1.48371
$R_0(\text{Si}_3-\text{H}_5)$	\AA	1.49070
$\angle_0(\text{O}_2-\text{H}_1-\text{Si}_3)$	deg	119.969
$\angle_0(\text{Si}_3-\text{O}_2-\text{H}_4)$	deg	106.489
$\angle_0(\text{Si}_3-\text{O}_2-\text{H}_5)$	deg	111.282
$R_e(\text{H}_1-\text{O}_2)$	\AA	0.95631
$R_e(\text{O}_2-\text{Si}_3)$	\AA	1.64771
$R_e(\text{Si}_3-\text{H}_4)$	\AA	1.47389
$R_e(\text{Si}_3-\text{H}_5)$	\AA	1.48160
$\angle_e(\text{O}_2-\text{H}_1-\text{Si}_3)$	deg	118.225
$\angle_e(\text{Si}_3-\text{O}_2-\text{H}_4)$	deg	105.768
$\angle_e(\text{Si}_3-\text{O}_2-\text{H}_5)$	deg	111.547

Table 4. Vibrationally averaged and equilibrium geometrical parameters of SiH_3NH_2

	Units	Value
$R_0(\text{H}_1-\text{Si}_2)$	\AA	1.49434
$R_0(\text{Si}_2-\text{N}_3)$	\AA	1.72495
$R_0(\text{Si}_2-\text{H}_4)$	\AA	1.48713
$R_0(\text{N}_3-\text{H}_6)$	\AA	0.98636
$\angle_0(\text{Si}_2-\text{H}_1-\text{N}_3)$	deg	114.848
$\angle_0(\text{Si}_2-\text{H}_5-\text{N}_3)$	deg	108.286
$\angle_0(\text{N}_3-\text{H}_6-\text{Si}_2)$	deg	121.756
$R_e(\text{H}_1-\text{Si}_2)$	\AA	1.48654
$R_e(\text{Si}_2-\text{N}_3)$	\AA	1.72159
$R_e(\text{Si}_2-\text{H}_4)$	\AA	1.47930
$R_e(\text{N}_3-\text{H}_6)$	\AA	1.00706
$\angle_e(\text{Si}_2-\text{H}_1-\text{N}_3)$	deg	115.666
$\angle_e(\text{Si}_2-\text{H}_5-\text{N}_3)$	deg	107.725
$\angle_e(\text{N}_3-\text{H}_6-\text{Si}_2)$	deg	119.860

berry et al. 2020). In fact, this bond length is even longer than the 1.67 \AA dative bond between NH_3 and BH_3 in ammonia borane (Thorne et al. 1983; Westbrook et al. 2021), suggesting that it also is dative in nature. SiH_3OH has an Si-O bond length of 1.65 \AA which is shorter than the Al-O bond length of 1.70 \AA in AlH_2OH and the Mg-O bond length of 1.77 \AA in HMgOH (Watrous et al. 2021). Despite the fact that Al-O has previously been reported to have a stronger bond than Mg-O or Si-O, (Doerksen & Fortenberry 2020) the slightly shorter bond length of Si-O compared to Al-O implies that Si-O has a stronger bond in these molecules. However, this is a small difference and the bond lengths of Si-O and Al-O are close to the same value. In SiH_3NH_2 , the Si-N bond has a length of 1.74 \AA which is smaller than the N-Mg bond length of 1.91 \AA in HMgNH_2 and slightly smaller than the Al-N bond length of 1.78 \AA in AlH_2NH_2 (Watrous et al. 2021). Just like with the aforementioned Si-O bond, the Si-N bond is shorter than the previously studied Al-N even though earlier work shows that the Al-N bond is stronger than the Si-N bond (Doerksen & Fortenberry 2020).

3.2 Vibrational Frequencies

Over half of the double-harmonic MP2/aug-cc-pVTZ intensities for AlH_3OH_2 , SiH_3OH , and Si_3NH_2 from Tables 5, 6, and 7 are on the same order or larger than the antisymmetric stretch in water, which

Table 5. Vibrational Frequencies (in cm⁻¹) of AlH₃OH₂ with MP2/aug-cc-pVTZ Intensities in Parentheses (in km mol⁻¹)

	Description	Harmonic	Anharmonic
ν_1 (a'')	1.001S ₁₁	3900.9 (142)	3715.0
ν_2 (a')	1.001S ₄	3801.2 (62)	3624.5
ν_3 (a')	0.952S ₁ +0.049S ₃	1920.4 (168)	1854.5
ν_4 (a')	0.951S ₃ -0.049S ₁	1881.9 (194)	1819.3
ν_5 (a'')	1.001S ₁₀	1871.5 (367)	1809.0
ν_6 (a')	0.622S ₈ +0.386S ₇	1649.2 (91)	1607.4
ν_7 (a'')	0.555S ₁₄ -0.394S ₁₅ -0.053S ₁₃	796.5 (261)	785.1
ν_8 (a')	0.475S ₉ -0.270S ₆ -0.159S ₈ -0.086S ₅	794.2 (297)	778.9
ν_9 (a')	0.461S ₆ +0.349S ₉ +0.186S ₅	777.0 (412)	775.3
ν_{10} (a'')	0.548S ₁₃ +0.430S ₁₂	713.4 (5)	664.0
ν_{11} (a')	0.540S ₅ +0.186S ₇ -0.159S ₆ -0.092S ₉	523.4 (153)	487.9
ν_{12} (a')	0.430S ₇ -0.192S ₅ -0.176S ₈ +0.116S ₆	386.5 (148)	319.7
ν_{13} (a')	1.016S ₂	372.6 (23)	350.6
ν_{14} (a'')	0.542S ₁₂ -0.369S ₁₃ -0.093S ₁₄	366.0 (5)	364.1
ν_{15} (a'')	0.613S ₁₅ +0.328S ₁₄	94.7 (37)	225.8

Table 6. Vibrational Frequencies (in cm⁻¹) of SiH₃OH with MP2/aug-cc-pVTZ Intensities in Parentheses (in km mol⁻¹)

	Description	Harmonic	Anharmonic
ν_1 (a')	0.999S ₁	3919.8 (82)	3742.9
ν_2 (a')	1.000S ₃	2286.9 (103)	2202.0
ν_3 (a')	1.001S ₄	2245.5 (87)	2167.4
ν_4 (a'')	1.001S ₉	2238.3 (162)	2159.1
ν_5 (a')	0.722S ₇ +0.192S ₆ -0.047S ₈	1007.8 (183)	990.6
ν_6 (a')	0.865S ₈ +0.065S ₆ -0.049S ₅	987.6 (113)	966.4
ν_7 (a'')	0.665S ₁₀ -0.304S ₁₂	967.9 (79)	952.3
ν_8 (a')	0.429S ₂ +0.341S ₅ +0.226S ₆	911.2 (70)	889.9
ν_9 (a')	0.521S ₂ -0.314S ₅ -0.094S ₆ +0.069S ₇	850.0 (126)	810.9
ν_{10} (a'')	0.961S ₁₁ -0.046S ₁₂	729.5 (60)	712.9
ν_{11} (a')	0.422S ₆ -0.286S ₅ -0.214S ₇ -0.077S ₈	690.1 (58)	683.3
ν_{12} (a'')	0.651S ₁₂ +0.342S ₁₀	196.2 (93)	181.1

has an intensity of roughly 70 km mol⁻¹. AlH₃OH₂, in particular, has four anharmonic frequencies with intensities over 200 km mol⁻¹, ν_5 , ν_7 , ν_8 , and ν_9 at 1809.0, 785.1, 778.9, and 775.3 cm⁻¹, respectively. These latter three are all within the 12-17 μ m region of the spectrum, making them particularly useful for potential detection of AlH₃OH₂ in this window. Further, of AlH₃OH₂'s five additional frequencies over 100 km mol⁻¹, ν_{11} is also close to this window with a frequency of 523.4 cm⁻¹ or 19.11 μ m.

The intense ν_5 antisymmetric Al-H stretching frequency at 1809.0 cm⁻¹ corresponds to 5.53 μ m which is in the range of the infrared typically associated with PAHs (Molster et al. 2001). This is quite a bit lower in frequency relative to the Ar matrix experimental value for the antisymmetric stretch of planar AlH₃ at 1882.7 cm⁻¹ (Kurth et al. 1993). Similarly, the observed value of the AlH₃ umbrella motion at 697.6 cm⁻¹ is substantially lower than that of the ν_9 O-Al-H bend in AlH₃OH₂ at 775.3 cm⁻¹ due to the water molecule's inhibition of this motion. In contrast, the experimental frequency of the bend in AlH₃ at 783.5 cm⁻¹ compares very well to the ν_8 H-O-Al-H torsion in AlH₃OH₂ which has a frequency of 778.9 cm⁻¹ implying a slight red-shift of this motion upon complexation with water.

SiH₃OH similarly has five anharmonic frequencies with intensities over 100 km mol⁻¹. Two of these, ν_2 and ν_4 , correspond to the symmetric and antisymmetric Si-H stretches. These frequencies at 2202.0 and 2159.1 cm⁻¹ are equivalent to 4.54 and 4.63 μ m respectively and are, again, at the end of the infrared spectrum typically associated with PAHs (Molster et al. 2001). Another frequency with a large intensity is ν_9 with an intensity of 126 km mol⁻¹ at 810.9 cm⁻¹ or 12.33 μ m. This frequency is mostly made of the Si-O stretch and is just within the 12-17 μ m region of the spectrum, making it a prime target for detection of this molecule. ν_{10} and ν_{11} also fall within this region at 712.9 and 683.3 cm⁻¹ or 14.03 and 14.63 μ m

Table 7. Vibrational frequencies (in cm⁻¹) of SiH₃NH₂ with MP2/aug-cc-pVTZ intensities (in km mol⁻¹) in parentheses

	Description	Harmonic	Anharmonic	Experiment ^a
ν_1 (a'')	1.001S ₁₁	3677.8 (22)	3515.3	3547
ν_2 (a')	1.000S ₄	3584.8 (15)	3438.7	3445
ν_3 (a'')	1.001S ₁₀	2258.0 (141)	2172.2	2172
ν_4 (a')	0.977S ₃	2256.1 (76)	2174.5	
ν_5 (a')	0.978S ₁	2208.9 (167)	2132.5	1564
ν_6 (a')	0.783S ₇ -0.218S ₈	1598.0 (29)	1563.7	
ν_7 (a')	0.517S ₆ +0.387S ₅ +0.078S ₉	1000.0 (215)	984.7	996
ν_8 (a'')	0.546S ₁₄ -0.334S ₁₅ -0.115S ₁₂	997.5 (65)	976.0	983
ν_9 (a')	0.903S ₉ -0.107S ₆	944.4 (103)	932.4	970
ν_{10} (a'')	0.623S ₁₃ -0.352S ₁₂	921.1 (40)	885.8	670 ^b
ν_{11} (a')	0.938S ₂	851.0 (49)	842.4	
ν_{12} (a')	0.612S ₅ -0.346S ₆ -0.072S ₉	712.8 (63)	699.2	670 ^b
ν_{13} (a'')	0.495S ₁₂ +0.368S ₁₃ +0.152S ₁₄	629.9 (35)	608.7	
ν_{14} (a')	0.833S ₈ +0.197S ₇ +0.044S ₉	393.4 (153)	244.2	
ν_{15} (a'')	0.683S ₁₅ +0.274S ₁₄	177.5 (13)	242.8	

^aFrom Ref. 6

^bRef. 6 points to both modes as potential identities for the peak at 670 cm⁻¹

respectively, although they have more modest intensities of 60 and 58 km mol⁻¹. Regardless, these frequencies may also help to elucidate the presence of SiH₃OH in this spectral window.

The SiH₃OH harmonic frequencies calculated in this work correspond well to previous CCSD(T)/d-aug-cc-pVTZ results (NIST 2020), with the largest difference occurring in ω_5 at just under 15 cm⁻¹. However, the average magnitude of the deviation is only 5.1 cm⁻¹. While there are no current experimental data for SiH₃OH, iso-valent CH₃OH is a well-known molecule in space (Ball et al. 1970; McGuire 2018) with comparable experimental data (Shimanouchi 1972). As such, the anharmonic frequencies of CH₃OH are also calculated at the F12-TZ level to serve as an additional benchmark for the data generated for the other molecules in this work. Of the 10 available gas-phase frequencies, the largest deviation occurs in ν_3 at a -54.0 cm⁻¹ difference between the experimental value of 2960 cm⁻¹ and the F12-TZ result at 2906.0 cm⁻¹. However, the computed O-H stretch has a difference of only 0.8 cm⁻¹ from the experimental data, and the average magnitude of the deviation is less than 10 cm⁻¹. This good overall agreement suggests the performance of the same methodology should provide accurate predictions of the fundamental frequencies of SiH₃OH, as well.

Like SiH₃OH, SiH₃NH₂ has five anharmonic frequencies with intensities over 100 km mol⁻¹. These are also the same types as the five most intense frequencies in AlH₃OH₂: the three third-row atom hydride stretches and two bends. The Si-H stretches fall just above the corresponding Si-H stretches of SiH₃OH at 4.60 and 4.69 μ m or 2174.5 and 2132.5 cm⁻¹. Additionally, the ν_{14} torsional fundamental at 244.2 cm⁻¹ or 40.95 μ m has an intensity of 153 km mol⁻¹. This frequency is significantly farther out from the infrared spectrum than the other frequency that has been attributed to silicates between 2.4 and 12 μ m (Molster et al. 2001), offering a new region for detecting such molecules at THz frequencies. The picture within the 12-17 μ m window is less vivid than for the other molecules, however. Only ν_{12} and ν_{13} fall directly within this region at 699.2 and 608.7 cm⁻¹ or 14.30 and 16.43 μ m, and they have fairly low intensities of 63 and 35 km mol⁻¹. ν_{11} also comes close to this window at 842.4 cm⁻¹ or 11.87 μ m, but it, too, has a modest intensity of only 49 km mol⁻¹. Still, all of these frequencies may help to shed some light on this currently sparsely-identified region of the spectrum.

The SiH₃NH₂ vibrational frequencies reported in this paper compare well to the available experimental data from Beach (1992). In particular, the computed ν_3 antisymmetric Si-H stretch at 2172.2 cm⁻¹ is virtually identical to the gas-phase value of 2172 cm⁻¹. However, the fairly broad peak in the experimental spectrum could

also be attributed to ν_4 , the symmetric Si-H stretch, or even ν_5 , the apical Si-H stretch, reported here to have very similar frequencies of 2174.5 and 2132.5 cm^{-1} . The proximity of these three modes would require a much more high-resolution experiment to separate them, but our methods are giving unique identification for this spectral region for this molecule. Similarly, ν_7 and ν_8 are assigned as shoulders on the more prominent ν_9 peak around 970 cm^{-1} in the experimental spectrum. In the same vein, the very broad peak centered around 670 cm^{-1} does not afford the opportunity to separate the distinct peaks reported here at 699.2 and 608.7 cm^{-1} for ν_{12} and ν_{13} , respectively. In all of these cases, direct attribution of the experimental spectrum is currently impossible, but the F12-TZ values presented herein may help to identify the unique spectral features of these modes in future high-resolution experiments.

The related SiO (Wilson et al. 1971; Dickinson 1972) and SiN (Turner 1992) molecules are well known in the interstellar medium and potentially offer a point of comparison for the Si-O stretch in SiH₃OH and the Si-N stretch in SiH₃NH₂. However, the Si-O stretch computed herein for SiH₃OH (again, ν_9) is substantially red-shifted compared to the experimental value for SiO at 1229.6 cm^{-1} (Huber & Herzberg 1979). Similarly, there is a large red-shift in the Si-N stretch in SiH₃NH₂ at 842.4 cm^{-1} compared to the experimental value for isolated SiN at 1138.4 cm^{-1} (Huber & Herzberg 1979). This suggests that even though the two pairs of molecules may be likely to occur in the same regions, they should have little spectral overlap. In fact, the closest SiH₃OH frequency to the SiO stretch is ν_5 at 990.6 cm^{-1} , and the closest SiH₃NH₂ frequency to the SiN stretch is ν_7 at 984.7 cm^{-1} , allowing SiH₃OH and SiH₃NH₂ to be easily disentangled spectroscopically from their related diatomic molecules, even if they are found in the same region. This is especially important for SiH₃OH in the case that it has a similar reduction pathway as carbon monoxide does to methanol.

Finally, ν_{15} for AlH₃OH₂ and SiH₃NH₂ both have positive anharmonicities. In particular, ν_{15} of AlH₃OH₂ shows quite a large positive anharmonicity of 131.1 cm^{-1} above the harmonic frequency, yielding a fundamental frequency of 225.8 cm^{-1} . The positive anharmonicity for SiH₃NH₂ is not as large with the anharmonic frequency at 242.8 cm^{-1} only 65.3 cm^{-1} above the harmonic frequency. While having such large positive anharmonicities raises questions about the reliability of the affected mode, it has been previously reported that near prolate molecules show positive anharmonicities in the smaller frequencies (McNavage et al. 2013; Fortenberry et al. 2012b,a; Huang et al. 2013; Watrous et al. 2021). These frequencies also have relatively small intensities, suggesting that they would be unhelpful for astronomical or laboratory detection anyway.

4 CONCLUSIONS

All three of the molecules examined in this work, AlH₃OH₂, SiH₃OH, and SiH₃NH₂, have substantial dipole moments that make them observable radioastronomically. In particular, AlH₃OH₂ has the largest dipole moment of the three at 4.58 D, while SiH₃OH and Si₃NH₂ have smaller dipoles at 1.29 and 1.21 D respectively. Each of these molecules also has at least five fundamental frequencies with large intensities greater than 100 km mol^{-1} , making the readily visible to infrared spectroscopic investigation, such as that performed by JWST or by the ongoing SOFIA mission. Nearly all of these intense modes are within the spectral range of the high-resolution EXES instrument on SOFIA, making it a particularly appealing avenue for taking advantage of the data presented herein. Even more importantly, each of these molecules has at least two frequencies within

the uncertain 12-17 μm spectral region, where identification may be particularly facile. For SiH₃NH₂ the frequencies in this region have intensities of only about 50 km mol^{-1} , but SiH₃OH has one frequency just inside this window at 12.33 μm with a substantial intensity of 126 km mol^{-1} . On the other hand, AlH₃OH₂ has three very intense frequencies in this region, with ν_7 , ν_8 , and ν_9 all having intensities above 261 km mol^{-1} , and ν_9 in particular having an enormous intensity of 412 km mol^{-1} . As such, AlH₃OH₂ may be particularly identifiable in this region.

Further, previous work has shown that AlH₃OH₂ is likely to be formed from reactions of water and the possible interstellar molecule of AlH₃ and may also provide insight into the formation of inorganic oxides from simple metal hydrides and water (Swinnen et al. 2009). Hence, the spectral data reported here will help with possible detection of this molecule through rotational and infrared spectroscopy, especially given the very large intensities of many of its fundamental frequencies and the occurrence of these frequencies in a relatively unidentified spectral region. Such a detection would help to shed some light on the abundance of the rotationally-dark AlH₃.

SiH₃OH and SiH₃NH₂ are similar to Al and Mg compounds that have been studied previously, and they both have highly intense vibrational frequencies in their own rights. Namely, the Si-O stretch in SiH₃OH at 850.0 cm^{-1} or 11.76 μm has an intensity of 126 km mol^{-1} , and the Si-H stretches of SiH₃NH₂ have intensities of 141, 76, and 167 km mol^{-1} at frequencies of 2258.0, 2256.1, and 2208.9 cm^{-1} or 4.429, 4.432, and 4.527 μm , respectively. Although these frequencies do not fall in the 12-17 μm region like some of the slightly less intense frequencies for these molecules, they are still found in a region of the spectrum in which few molecules have currently been identified and those that have been elucidated are primarily carbonaceous molecules like PAHs. Hence, the present work may help to shed some light on new types of molecules that are waiting to be found in this region of the spectrum as well.

ACKNOWLEDGEMENTS

This work is made possible by NASA Grant NNX17AH15G, NSF Grant OIA-1757220, and the College of Liberal Arts at the University of Mississippi. The computational facilities were provided by the Mississippi Center for Supercomputer Research (MCSR).

DATA AVAILABILITY

Supplementary data are available at MNRAS online.

Table S1. CCSD(T)-F12b/cc-pVTZ-F12 equilibrium and first vibrationally-excited rotational constants for AlH₃OH₂, SiH₃NH₂, and SiH₃OH (in MHz).

Table S2. Fermi Resonances of AlH₃OH₂, SiH₃OH, and SiH₃NH₂.

REFERENCES

- Adler T. B., Knizia G., Werner H.-J., 2007, *J. Chem. Phys.*, 127, 221106
 Agbaglo D., Fortenberry R. C., 2019a, *Int. J. Quantum Chem.*, 119, e25899
 Agbaglo D., Fortenberry R. C., 2019b, *Chem. Phys. Lett.*, 734, 136720
 Allen W. D., coworkers 2005
 Ball J. A., Gottlieb C. A., Lilley A. E., Radford H. E., 1970, *Astrophys. J. Lett.*, 162, L203
 Beach D. B., 1992, *Inorg. Chem.*, 31, 4174
 Chubb K. L., Min M., Kawashima Y., Helling C., Waldmann I., 2020, *Astronom. Astrophys.*, 639

- Crawford T. D., Schaefer III H. F., 2000, in Lipkowitz K. B., Boyd D. B., eds., Vol. 14, *Reviews in Computational Chemistry*. Wiley, New York, pp 33–136
- Dickinson D. F., 1972, *Astrophys. J.*, 175, L43
- Doerksen E. S., Fortenberry R. C., 2020, *ACS Earth Space Chem.*, 4, 812
- Fortenberry R. C., Lee T. J., 2019, *Ann. Rep. Comput. Chem.*, 15, 173
- Fortenberry R. C., Huang X., Francisco J. S., Crawford T. D., Lee T. J., 2012a, *J. Phys. Chem. A.*, 116, 9582
- Fortenberry R. C., Huang X., Francisco J. S., Crawford T. D., Lee T. J., 2012b, *J. Chem. Phys.*, 136, 234309
- Fortenberry R. C., Trabelsi T., Francisco J. S., 2020, *J. Phys. Chem. A*
- Frisch M. J., et al., 2016, *Gaussian-16 Revision C.01*
- Gaw J. F., Willets A., Green W. H., Handy N. C., 1996
- Huang X., Fortenberry R. C., Lee T. J., 2013, *J. Chem. Phys.*, 139, 084313
- Huber K. P., Herzberg G., 1979, *Constants of Diatomic Molecules*. Springer Science+Business Media New York
- Kendall R. A., Dunning T. H., Harrison R. J., 1992, *J. Chem. Phys.*, 96, 6796
- Knizia G., Adler T. B., Werner H.-J., 2009, *J. Chem. Phys.*, 130, 054104
- Kurth F. A., Eberlein R. A., Schnöckel H., Downs A. J., Pulham C. R., 1993, *J. Chem. Soc., Chem. Commun.*, pp 1302–1304
- Martin J. M. L., Taylor P. R., 1997, *Spectrochim. Acta A*, 53, 1039
- Martin J. M. L., Lee T. J., Taylor P. R., François J.-P., 1995, *J. Chem. Phys.*, 103, 2589
- McGuire B. A., 2018, *Astrophys. J. Suppl. Ser.*, 239, 17
- McGuire B. A., Burkhardt A. M., Kalenskii S., Shingledecker C. N., Remijan A. J., Herbst E., McCarthy M. C., 2018, *Science*, 359, 202
- McNavage W., Wilhelm M. J., Dai H.-L., 2013, *Chem. Phys.*, 422, 290
- Mills I. M., 1972, in Rao K. N., Mathews C. W., eds., *Molecular Spectroscopy - Modern Research*. Academic Press, New York, pp 115–140
- Møller C., Plesset M. S., 1934, *Phys. Rev.*, 46, 618
- Molster F. J., et al., 2001, *Astron. Astrophys.*, 372, 165
- Molster F. J., Waters L. B. F. M., Tielens A. G. G. M., 2002, *Astronom. Astrophys.*, 382, 222
- NIST 2020, NIST Computational Chemistry Comparison and Benchmark Database
- Papoušek D., Aliev M. R., 1982, *Molecular Vibration-Rotation Spectra*. Elsevier, Amsterdam
- Peterson K. A., Adler T. B., Werner H.-J., 2008, *J. Chem. Phys.*, 128, 084102
- Raghavachari K., Trucks G. W., Pople J. A., Replogle E., 1989, *Chem. Phys. Lett.*, 158, 207
- Savage B. D., Sembach K. R., 1996, *Annu. Rev. Astron. Astrophys.*, 34, 279
- Shavitt I., Bartlett R. J., 2009, *Many-Body Methods in Chemistry and Physics: MBPT and Coupled-Cluster Theory*. Cambridge University Press, Cambridge
- Shimanouchi T., 1972, *Tables of Molecular Vibrational Frequencies*, 39th edn. Vol. 1, National Standards Reference Data System, Washington, DC
- Swinen S., Nguyen V. S., Sakai S., Nguyen M. T., 2009, *Chem. Phys. Lett.*, 472, 175
- Takigawa A., Kamizuka T., Tachibana S., Yamamura I., 2017, *Sci. Adv.*, 3
- Tenenbaum E. D., Ziurys L. M., 2009, *Astrophys. J.*, 693, L59
- Tenenbaum E. D., Ziurys L. M., 2010, *Astrophys. J.*, pp L93–L97
- Thorne L. R., Suenram R. D., Lovas F. J., 1983, *J. Chem. Phys.*, 78, 167
- Turner B. E., 1992, *Astrophys. J.*, 388, L35
- Valencia E. M., Worth C. J., Fortenberry R. C., 2020, *Mon. Not. Royal Astron. Soc.*, 492, 276
- Watrous A. G., Davis M. C., Fortenberry R. C., 2021, *Frontiers in Astronomy and Space Sciences*, 8
- Watson J. K. G., 1977, in Doring J. R., ed., *Vibrational Spectra and Structure*. Elsevier, Amsterdam, pp 1–89
- Werner H.-J., et al., 2015
- Werner H.-J., et al., 2020
- Westbrook B. R., Fortenberry R. C., 2020, *J. Phys. Chem. A*, 124, 3191
- Westbrook B. R., Valencia E. M., Rushing S. C., Tschumper G. S., Fortenberry R. C., 2021, *J. Chem. Phys.*, 154, 041104
- Wilson R. W., Penzias A. A., Jefferts K. B., Kutner M., Thaddeus P., 1971, *Astrophys. J.*, 167, L97
- Yousaf K. E., Peterson K. A., 2008, *J. Chem. Phys.*, 129, 184108

REFERENCES

- Adler T. B., Knizia G., Werner H.-J., 2007, *J. Chem. Phys.*, 127, 221106
- Agbaglo D., Fortenberry R. C., 2019a, *Int. J. Quantum Chem.*, 119, e25899
- Agbaglo D., Fortenberry R. C., 2019b, *Chem. Phys. Lett.*, 734, 136720
- Allen W. D., coworkers 2005
- Ball J. A., Gottlieb C. A., Lilley A. E., Radford H. E., 1970, *Astrophys. J. Lett.*, 162, L203
- Beach D. B., 1992, *Inorg. Chem.*, 31, 4174
- Chubb K. L., Min M., Kawashima Y., Helling C., Waldmann I., 2020, *Astronom. Astrophys.*, 639
- Crawford T. D., Schaefer III H. F., 2000, in Lipkowitz K. B., Boyd D. B., eds., Vol. 14, *Reviews in Computational Chemistry*. Wiley, New York, pp 33–136
- Dickinson D. F., 1972, *Astrophys. J.*, 175, L43
- Doerksen E. S., Fortenberry R. C., 2020, *ACS Earth Space Chem.*, 4, 812
- Fortenberry R. C., Lee T. J., 2019, *Ann. Rep. Comput. Chem.*, 15, 173
- Fortenberry R. C., Huang X., Francisco J. S., Crawford T. D., Lee T. J., 2012a, *J. Phys. Chem. A.*, 116, 9582
- Fortenberry R. C., Huang X., Francisco J. S., Crawford T. D., Lee T. J., 2012b, *J. Chem. Phys.*, 136, 234309
- Fortenberry R. C., Trabelsi T., Francisco J. S., 2020, *J. Phys. Chem. A*
- Frisch M. J., et al., 2016, *Gaussian-16 Revision C.01*
- Gaw J. F., Willets A., Green W. H., Handy N. C., 1996
- Huang X., Fortenberry R. C., Lee T. J., 2013, *J. Chem. Phys.*, 139, 084313
- Huber K. P., Herzberg G., 1979, *Constants of Diatomic Molecules*. Springer Science+Business Media New York
- Kendall R. A., Dunning T. H., Harrison R. J., 1992, *J. Chem. Phys.*, 96, 6796
- Knizia G., Adler T. B., Werner H.-J., 2009, *J. Chem. Phys.*, 130, 054104
- Kurth F. A., Eberlein R. A., Schnöckel H., Downs A. J., Pulham C. R., 1993, *J. Chem. Soc., Chem. Commun.*, pp 1302–1304
- Martin J. M. L., Taylor P. R., 1997, *Spectrochim. Acta A*, 53, 1039
- Martin J. M. L., Lee T. J., Taylor P. R., François J.-P., 1995, *J. Chem. Phys.*, 103, 2589
- McGuire B. A., 2018, *Astrophys. J. Suppl. Ser.*, 239, 17
- McGuire B. A., Burkhardt A. M., Kalenskii S., Shingledecker C. N., Remijan A. J., Herbst E., McCarthy M. C., 2018, *Science*, 359, 202
- McNavage W., Wilhelm M. J., Dai H.-L., 2013, *Chem. Phys.*, 422, 290
- Mills I. M., 1972, in Rao K. N., Mathews C. W., eds., *Molecular Spectroscopy - Modern Research*. Academic Press, New York, pp 115–140
- Møller C., Plesset M. S., 1934, *Phys. Rev.*, 46, 618
- Molster F. J., et al., 2001, *Astron. Astrophys.*, 372, 165
- Molster F. J., Waters L. B. F. M., Tielens A. G. G. M., 2002, *Astronom. Astrophys.*, 382, 222
- NIST 2020, NIST Computational Chemistry Comparison and Benchmark Database
- Papoušek D., Aliev M. R., 1982, *Molecular Vibration-Rotation Spectra*. Elsevier, Amsterdam
- Peterson K. A., Adler T. B., Werner H.-J., 2008, *J. Chem. Phys.*, 128, 084102
- Raghavachari K., Trucks G. W., Pople J. A., Replogle E., 1989, *Chem. Phys. Lett.*, 158, 207
- Savage B. D., Sembach K. R., 1996, *Annu. Rev. Astron. Astrophys.*, 34, 279
- Shavitt I., Bartlett R. J., 2009, *Many-Body Methods in Chemistry and Physics: MBPT and Coupled-Cluster Theory*. Cambridge University Press, Cambridge
- Shimanouchi T., 1972, *Tables of Molecular Vibrational Frequencies*, 39th edn. Vol. 1, National Standards Reference Data System, Washington, DC
- Swinen S., Nguyen V. S., Sakai S., Nguyen M. T., 2009, *Chem. Phys. Lett.*, 472, 175
- Takigawa A., Kamizuka T., Tachibana S., Yamamura I., 2017, *Sci. Adv.*, 3
- Tenenbaum E. D., Ziurys L. M., 2009, *Astrophys. J.*, 693, L59
- Tenenbaum E. D., Ziurys L. M., 2010, *Astrophys. J.*, pp L93–L97
- Thorne L. R., Suenram R. D., Lovas F. J., 1983, *J. Chem. Phys.*, 78, 167
- Turner B. E., 1992, *Astrophys. J.*, 388, L35
- Valencia E. M., Worth C. J., Fortenberry R. C., 2020, *Mon. Not. Royal Astron. Soc.*, 492, 276
- Watrous A. G., Davis M. C., Fortenberry R. C., 2021, *Frontiers in Astronomy*

- and Space Sciences, 8
Watson J. K. G., 1977, in Doring J. R., ed., , *Vibrational Spectra and Structure*.
Elsevier, Amsterdam, pp 1–89
Werner H.-J., et al., 2015
Werner H.-J., et al., 2020
Westbrook B. R., Fortenberry R. C., 2020, *J. Phys. Chem. A*, 124, 3191
Westbrook B. R., Valencia E. M., Rushing S. C., Tschumper G. S., Fortenberry
R. C., 2021, *J. Chem. Phys.*, 154, 041104
Wilson R. W., Penzias A. A., Jefferts K. B., Kutner M., Thaddeus P., 1971,
Astrophys. J., 167, L97
Yousaf K. E., Peterson K. A., 2008, *J. Chem. Phys.*, 129, 184108

This paper has been typeset from a $\text{\TeX}/\text{\LaTeX}$ file prepared by the author.